

P_D SO tuning of PFC-SAC fault tolerant flight control system

Andrea Alaimo^a, Antonio Esposito^b and Calogero Orlando^{*}

Faculty of Engineering and Architecture, Kore University of Enna, Cittadella Universitaria, 94100, Enna, Italy

(Received November 5, 2018, Revised March 3, 2019, Accepted March 4, 2019)

Abstract. In the design of flight control systems there are issues that deserve special consideration and attention such as external perturbations or systems failures. A Simple Adaptive Controller (SAC) that does not require a-priori knowledge of the faults is proposed in this paper with the aim of realizing a fault tolerant flight control system capable of leading the pitch motion of an aircraft. The main condition for obtaining a stable adaptive controller is the passivity of the plant; however, since real systems generally do not satisfy such requirement, a properly defined Parallel Feedforward Compensator (PFC) is used to let the augmented system meet the passivity condition. The design approach used in this paper to synthesize the PFC and to tune the invariant gains of the SAC is the Population Decline Swarm Optimization (P_D SO). It is a modification of the Particle Swarm Optimization (PSO) technique that takes into account a decline demographic model to speed up the optimization procedure. Tuning and flight mechanics results are presented to show both the effectiveness of the proposed P_D SO and the fault tolerant capability of the proposed scheme to control the aircraft pitch motion even in presence of elevator failures.

Keywords: simple adaptive control; population decline swarm optimizer; parallel feedforward compensator; fault tolerant control

1. Introduction

The modern digital electronic control system as fly by wire has become a standard for the civil aircraft leading to an increase in term of safety and performance. In the last decades the complexity of such flight control systems has been increasing more and more and, as a consequence, the requirement for safety, reliability, maintainability, and survivability has increased as well (Favre (1994), Liu *et al.* (2018)). It stems the need to design control systems capable of tolerating potential faults. For such reason, the integrated strategy of fault-tolerant control system (FTCS) has been widely studied and developed. A FTCS must have the ability to automatically handle a system fault and be able to maintain overall system stability and acceptable performance in the event of such failures.

^{*}Corresponding author, Ph.D., E-mail: calogero.orlando@unikore.it

^aPh.D., E-mail: andrea.alaimo@unikore.it

^bPh.D., E-mail: antonio.esposito@unikore.it

Generally speaking, FTCS can be classified in two groups: passive (PFTCS) and active (AFTCS). The PFTCS controllers are fixed and designed to be robust against a class of considered faults (Eterno *et al.* (1985)). On the other hand, AFTCS react to system component failures actively by reconfiguring control actions (Steinberg (2005)), so that the stability and acceptable performance of the entire system can be maintained. Starting from the accessible information after system fault, a reconfigurable controller should be designed to maintain stability, steady state and desired dynamic performance (Zhang and Jiang (2008)). In particular, in the presence of an actuator, to avoid saturation and to take into account reduced performance, it may also be necessary to design a reference/command regulator to automatically adjust the command input (Zhang and Jiang (2003)). Some works on FTCS design are based on the idea of recovering system performance as much as possible with respect to the unbroken system (Noura *et al.* (2000), Wise *et al.* (1999), Zhang and Jiang (2002)). However, in practice, in the event of an actuator fault, the available capabilities of the actuator could be significantly reduced. Thus if the design goal is to maintain the original system performance, this may force the remaining actuators to work beyond the normal duty to compensate for disadvantages caused by the error. Clearly, this situation has to be avoided in practice, due to the physical limitations of the actuators. An FTCS designed in this way can lead to saturation of the actuator or, even worse, cause further damage. Therefore, the compromise between the achievable performance and the available capacity of the actuator should be wisely considered.

Regarding the design methods, a detailed classification can be made according to (Zhang and Jiang (2007), Zhang and Jiang (2008)) by taking into account one of the following four criteria: (1) mathematical design tools; (2) design approaches; (3) reconfiguration mechanisms; and (4) linear or nonlinear systems type. The adaptive control method used in this work belongs to the first group. An Adaptive Control is based on control laws that autonomously modify their parameters to adapt to the system variations. Different Adaptive Control techniques have been developed to overcome the changes that the system may undergo during the exercise of its functions. Among these, the Model Reference Adaptive Control (MRAC) has been extensively investigated (Goodwin and Sin (2014), Ioannou *et al.* (1996), Landau *et al.* (1998), Tao (2003)). The main feature of a MRAC is that it incorporates a reference model which represents the desired input-output behavior. The control objective for the plant output and adaptation law are designed to force the response of the plant to follow the behavior of the reference model for any given reference input (Gertler (2013)).

To control high order systems where the order of the controller cannot be close to the order of the state of the plant, it was necessary to design low-order controllers. These low-order adaptive controllers were considered to be modest replicas of regular MRACs. However, recent results seem to show that such low-order adaptive controllers not only do not provide reduced performance, but on the contrary, they could be the right approach Barkana (2014). Simple Adaptive Control (SAC), for instance, is a reduced order control method that is claimed to be "a stable direct model reference adaptive control methodology", see (Sobel *et al.* (1979), Barkana *et al.* (1983), Barkana (2014)). As example applications of the SAC controller the following may be cited: (Barkana and Kaufman (1985)) applied the method

to control unstable helicopters and missile showing stability and boundedness of errors and states for minimum phase systems; (Morse and Ossman (1990)) studied a reconfigurable flight control system for the AFTI/F-16 proving the capability of the control system to maintain the desired performance of the linearized plant in presence of quadruple failures; (Barkana and Kaufman (1993)) and (Min *et al.* (2012)) showed the applicability of SAC and adaptive backstepping SAC to control large flexible spacecraft structures; (Barkana (2005)) proposed the combination of classical and simple adaptive controller to stabilize first and then to meet the desired performance of a nonminimum phase autopilot system; (Ulrich and Lafontaine (2007)) analyzed a simplified SAC algorithm to let a fighter aircraft behave like a conventional aircraft; (Omori *et al.* (2013)) investigated numerically and experimentally the fault tolerant ability of a flight control system based on the combined use of SAC and classical PID controllers; (Rusnak and Barkana (2014)) presented an add-on SAC based method to improve the controlling performance of missile autopilot; (Chen *et al.* (2015)) proposed the use of SAC in conjunction with a quantum logic approach to obtain a good tracking capability for a quadrotor helicopter in presence of failures that reduces the effectiveness of propellers; (Gransden and Mooij (2016)) used the SAC technology to control a rigid satellite equipped with flexible solar arrays; (Takase *et al.* (2017)) presented the use of PID-SAC to manage the pilot pitch control considering the human pilot in the loop; (Matsuki *et al.* (2018)) extending previous works, investigated the fault tolerant capability of PID-SAC control of aircraft motion.

More in detail, the SAC is a simplification of MRAC that do not requested neither for full state feedback nor for online parameters identifications of the controlled plant. The output of the plant to be controlled should track a reference signal which is generated by a reference model that represents the ideal behavior that the controlled plant should manifest. Two main difficulties arise: *i*) the transfer function of the plant to be controlled should meet at least the Almost Strictly Positive Realness (ASPR) condition and *ii*) the invariant weight coefficients of the SAC scheme should be properly determined (Ulrich and Lafontaine (2007)). In particular, the first aforementioned point is such that almost none real system meets ASPR condition. The problem can be tackled by synthesizing a Parallel Feedforward Compensator (PFC) such that the augmented plant satisfies the ASPR requirements (Barkana (2014)).

In this paper an alternative scheme for tuning both the parallel feedforward compensator and the SAC parameters is proposed and verified. The approach is based on particle swarm optimization, (Clerc and Kennedy (2002)), modified in such a way to increase the search capability of the swarm reducing at the same time the computational effort. This is achieved by introducing a population decline model (Orlando and Alaimo, 2017) that allows to start the exploration phase with a large swarm which is reducing moving toward the exploitation phase. For such reason the obtained approach has been named *P_DSO* - Population Decline Swarm Optimizer. The adaptive control scheme tuned by the proposed optimization procedure is last applied to aircraft longitudinal stabilization and control even in presence of fault.

The Paper is organized as follows: section 2 briefly introduces the adaptive control scheme and presents the aircraft longitudinal model and the study cases; section 3 describes the proposed *P_DSO* - Population Decline Swarm Optimizer and the controller tuning rules; the

controller design results are given in section 4 while section 5 collects validation and case studies simulation results; last, paper conclusion are summarized in section 6.

2. PFC-SAC longitudinal control system and study cases

Let us assume that the plant is modeled by a controllable and observable SISO linear system given by

$$\begin{aligned}\dot{\mathbf{x}}(t) &= \mathbf{A}\mathbf{x}(t) + \mathbf{b}u(t) \\ y(t) &= \mathbf{c}^T \mathbf{x}(t)\end{aligned}\quad (1)$$

where \mathbf{x} is the n -dimensional real state vector, \mathbf{A} is the $n \times n$ dynamic matrix, \mathbf{b} and \mathbf{c} are the input and output vector (superscript T labels transposition), respectively, while y and u are the output and input signals. The plant Eq. 1 is requested to follow a stable reference model that writes as

$$\begin{aligned}\dot{\mathbf{x}}_m(t) &= \mathbf{A}_m \mathbf{x}_m(t) + \mathbf{b}_m u_m(t) \\ y_m(t) &= \mathbf{c}_m^T \mathbf{x}_m(t)\end{aligned}\quad (2)$$

being \mathbf{x}_m the n -dimensional reference model state vector, $\{\mathbf{A}_m, \mathbf{b}_m, \mathbf{c}_m\}$ are the model reference system matrices and y_m and u_m are the output and bounded input signals of the reference model.

The idea of Simple Adaptive Control stems from the consideration that, for stability of adaptive control systems, the plant is required to be stabilizable via a constant gain feedback. Thus, the adaptive algorithm, which is very similar to the usual MRAC algorithms, is then augmented with an additional adaptive output feedback term (Barkana (2014)). In particular, the control input is a linear combination of the model reference state \mathbf{x}_m , of the model input u_m and of the output tracking error $e(t) = y(t) - y_m(t)$ and it writes as

$$u(t) = \mathbf{K}^T(t) \mathbf{r}(t) \quad (3)$$

where $\mathbf{r}^T = [e, \mathbf{x}_m, u_m]$ is the reference vector while $\mathbf{K}^T = [K_e, \mathbf{K}_{xm}, K_{um}]$ is the adaptive gain vector that is defined by the following relations

$$\mathbf{K} = \mathbf{K}_P + \mathbf{K}_I \quad (4)$$

$$\mathbf{K}_P = e\mathbf{\Gamma}\mathbf{r} \quad (5)$$

$$\dot{\mathbf{K}}_I + \sigma\mathbf{K}_I = e\mathbf{\Gamma}\mathbf{r} \quad (6)$$

with $\mathbf{\Gamma}$ a diagonal matrix that collects the SAC invariant gains Γ_e, Γ_{xm} and Γ_{um} , while the invariant σ is introduced to guarantee stability with respect to boundedness in presence of disturbances (Barkana (2017)).

The SAC thus takes into account the tracking error, the model states and the model input to generate the adaptive control input that leads the plant. Differently from the standard MRAC, it is not requested to the reference model Eq.2 to reproduce the plant (for instance,

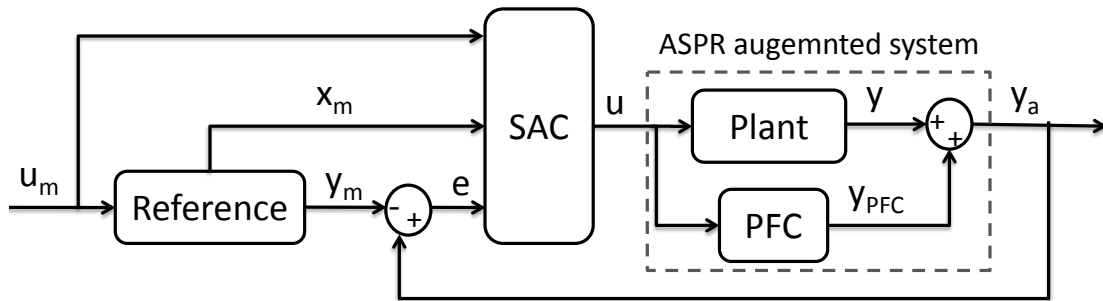


Fig. 1 PFC augmented system controlled by SAC

the reference model could be just a first order or higher order system), it is only requested to generate the desired trajectory. It follows that there is no unmodeled dynamics since there is no need to compare the model and the plant (Barkana (2014)). Moreover, the architecture of SAC is simpler than that of conventional MRAC since only output feedback is used and there is no need for the construction of a plant state observer.

It is now worth stating that the main condition requested to obtain a stable adaptive control, despite of the variation of the adaptive controller gains, is the passivity of the plant which means that the plant transfer function is Almost Strictly Positive Real (ASPR). However, almost all real systems are not ASPR and it is thus needed to tackle such issue to implement the simple adaptive controller. The method proposed by (Barkana (1987)), that asks for the implementation of a PFC - parallel feedforward compensator to allow the transfer function of the augmented systems meeting the ASPR condition, is here employed. Figure 1 shows the PFC augmented system controlled by the SAC while the augmented system transfer function G_a reads as

$$G_a(s) = G_0(s) + G_{PFC}(s) \tag{7}$$

being G_0 the plant transfer function and G_{PFC} the parallel feedforward compensator transfer function.

More in detail, a system transfer function $G(s)$ is said to be ASPR if there exist a constant gain K such that the closed loop transfer function $G_{cl} = G(s)/\{1 + KG(s)\}$ is stable and $\Re\{G_{cl}(j\omega)\} > 0$ for $-\infty < \omega < \infty$. This also implies that the phase of the system transfer function $\angle G_{cl}(s)$ is not too high at low frequencies and that its absolute value is lower than 90 deg at high frequencies, for more details the interested reader can see the work of Rusnak and Barkana (2009). In other words, the aforementioned conditions for a SISO system imply that if the transfer function is minimum phase (all zeros in the left half complex plane), its relative degree is 1 and the numerator leading coefficient is positive then the system transfer function meets ASPR requirements.

Moreover, it is to be said here that a potential drawback of applying the parallel feedforward scheme to render the controlled system ASPR is that the actual control variable is the output of the augmented system, see Figure 1. It is thus important to design the PFC such that its influence on the system output is as small as possible, namely $y_a = y + y_{PFC} \approx y$.

The last condition on small influence specifies in the existence of frequency ω^* such that $G_a(j\omega) \approx G(j\omega)$ for $0 \leq \omega \leq \omega^*$.

In order to apply the aforementioned approach to realize a fault tolerant flight control system, a simplified model of an aircraft longitudinal behavior is considered and advantage is taken of the population decline swarm optimizer $P_{D}SO$ (Orlando and Alaimo (2017)) for tuning parallel feedforward compensator (PFC) and the invariant gains of the simple adaptive controller (SAC). The aircraft model used in this work is taken from literature (Omori *et al.* (2013); Tokunaga *et al.* (2015); Nishiyama *et al.* (2016)) and has already been used to study a flight control system based on a combination of SAC and PID. Equations are here reported for the sake of completeness. The aircraft longitudinal dynamic is linearized about the steady level flight trim conditions given by true airspeed $TAS = 66.5 m/s$ and angle of attack $AOA = 4.98 deg$ at an altitude of $1524 m$ while the thrust is maintained constant. The plant is modeled as a Single Input Single Output (SISO) system while the objective of PFC-SAC system is to control the aircraft pitch angle variation with respect to trim condition, θ , by commanding the elevator angle δ_e . The transfer function (Omori *et al.* (2013)) of the modeled aircraft longitudinal dynamic writes as

$$G_0(s) = \frac{\theta}{\delta_e} = \frac{4.22s^2 + 4.31s + 0.212}{s^4 + 3.01s^3 + 6.96s^2 + 0.232s + 0.224} \quad (8)$$

In all the investigated study cases described in what follows, the elevator is commanded using a smoothed square wave which is modeled as

$$\delta_c = \frac{2A_{ssw}}{\pi} \tan^{-1} [\rho_{ssw} \sin(2\pi f_{ssw}t)] \quad (9)$$

being A_{ssw} and f_{ssw} the amplitude and frequency of the smoothed square wave while ρ_{ssw} is a parameter that governs the square wave smoothing radius.

More in detail, two study cases are taken into account to design and verify the proposed control system. The first case study deals with the nominal model Eq. 8 and it is referred to as Nominal. It is used to tune the invariant parameters of the simple adaptive control scheme, Γ_e , Γ_{xm} and Γ_{um} and to verify the SAC behavior in the fault free condition. On the other hand, the second study case represents a fault scenario that is considered to test the fault-tolerant capability of the designed PFC-SAC controller (Omori *et al.* (2013)). The second study case takes into account a sudden reduction of elevator effectiveness during flight. The loss of elevator effectiveness can be due to different causes among which one can cite the formation of ice on the horizontal stabilizer (Miller and Ribbens (1999)) or actuator failures (Gai and Wang (2013)), for instance. It is assumed that at the time t_{ef} the effectiveness of the elevator becomes λ_{ef} times that of the fault free model. In the case that the elevator effectiveness reduces, the aircraft system transfer function writes as

$$G_{ef}(s) = \lambda_{ef}G_0 \quad (10)$$

where the subscript ef stands for elevator fail and $0 < \lambda_{ef} \leq 1$.

3. *P_DSO* control system design

In order to design the components of the SAC controller scheme, suitable scalar indexes that quantify the achievement of particular design objectives are introduced. Each index, one for the PFC design problem and one for the SAC parameters tuning, represents a fitness function to be minimized by the optimization procedure. The alternative Population Decline Swarm Optimization method proposed to design the PFC and to select the best invariant parameters of the SAC controller is described in the present section starting from its foundation that is the PSO scheme (Shi and Eberhart (1998)).

More in detail, the fundamental of the particle swarm optimization technique relies upon a simplified social model of a swarm of birds that is looking for food. Each individual, a particle, is at first randomly located in the search space by means of an n -dimensional vector called position variable. The procedure then solves the problem under consideration for each particle and evaluate an *a priori* chosen objective function looking for its minimum value. At successive steps, each particle moves in accordance with the swarm toward the current global best solution and at the same time accelerates toward its own personal previous best solution. These two movements are referred to as social and cognitive accelerations and depend on the distance between the current position of the particle and global and personal best solutions through random weights. The process goes on until the maximum number of allowed iterations is met or a convergence condition is fulfilled.

It is worth noting that, every time that the parameters to be selected are modified by the optimization procedure, the dynamic response of the controlled system has to be computed under the chosen design conditions to compute the value of the fitness function.

This implies that the computational effort increases with the number of particles in the swarm and thus slowing down the optimization procedure. It is however to evidence that as the number of particles increases the exploration capability of the swarm enhances as well. On the contrary, when a small size swarm is employed then the procedure speeds up; the drawback is that the probability that the swarm locks into a local minimum becomes high.

Another characteristic drawback common to optimization algorithms based on simplified social behavior or natural evolution models is related to the random initialization of the swarm in the search space and to the stochastic nature of such optimization schemes: namely, different swarms find different minimum points when the same optimization problem is solved. This means that probability to stuck into local minima is always present despite of the swarm dimension. A method proposed in literature (Marti (2003)) to address such problem is the so-called Multi-Start technique that foreseen multiple re-initialization of the swarm during the global minimum searching steps.

The population decline particle swarm optimizer *P_DSO* proposed here has the purpose to enhance the overall performance of the standard PSO (Shi and Eberhart, 1998) in a twofold ways: *i*) to increase the exploration capability by using a large size swarm during the initialization and the first iteration steps; *ii*) to speed up the procedure by continuously reducing the number of particles in the swarm during the exploitation phase.

First the *P_DSO* procedure is presented, then the fitness functions to be minimized looking for the PFC and SAC tuning, respectively, are described.

3.1 Population decline swarm optimizer

Let us assume that a swarm of particles is used to search for the global minimum of the objective function \mathfrak{S} using the PSO approach (Shi and Eberhart, 1998) and let assume that the population size at the first iteration step, i.e. at the initialization stage, is P_{max} and that each particle in the present study is represented by a n -dimensional position variables vector defined as p_λ^i with $i = 1, 2, \dots, P_\lambda$, being P_λ the swarm size at the iteration step λ . At first the swarm is randomly initialized and at the successive steps each particle position is updated as

$$p_{\lambda+1}^i = p_\lambda^i + v_{\lambda+1}^i \quad (11)$$

where $\lambda = 1, 2, \dots, \Lambda$ is the iteration step and Λ is the maximum number of iterations. In Eq. 11, $v_{\lambda+1}^i$ is the updated particle velocity which reads as

$$v_{\lambda+1}^i = \chi [\mu_\lambda v_\lambda^i + c_c r_1 (p_b^i - p_\lambda^i) + c_s r_2 (p_b^g - p_\lambda^i)] \quad (12)$$

where c_c and c_s are accelerations coefficients that are called cognitive and social constants, respectively. The former is in fact responsible of the particle acceleration toward the previous personal best position p_b^i while the latter accelerates the particle toward the previous best position attained by any of the particle of the swarm p_b^g . In Eq. 12, r_1 and r_2 are random numbers in the interval $[0, 1]$ while the term μ_λ , called inertia weight (Shi and Eberhart, 1998), is used to balance the global and the local search and varies linearly between minimum and maximum values (generally set in literature to 0.4 and 0.9, respectively) as

$$\mu_\lambda = \mu_{max} \left(1 - \frac{\lambda}{\Lambda}\right) + \mu_{min} \frac{\lambda}{\Lambda} \quad (13)$$

The only parameter that appears in Eq. 12, which is yet to be defined, is the constriction factor χ . It aims at preventing the swarm explosion ensuring the convergence and writes as (Clerc and Kennedy, 2002; Marinaki *et al.*, 2011)

$$\chi = \frac{2}{\left|2 - \varphi - \sqrt{\varphi^2 - 4\varphi}\right|} \quad \text{with} \quad \varphi = c_c + c_s > 4 \quad (14)$$

Last, a stepwise population decline model is introduced to modify the PSO procedure in such a way to increase the swarm search capability during initial stages and to constantly accelerate the searching procedure as iteration goes on. The population decline model writes as

$$P_\lambda = \begin{cases} P_{max} & \lambda = 1 \\ \lceil P_{\lambda-1} \xi \rceil & \text{if } \frac{\lambda}{\Delta} = \lfloor \frac{\lambda}{\Delta} \rfloor \\ P_{\lambda-1} & \text{otherwise} \end{cases} \quad (15)$$

where Δ , called time for population decline, is the number of iterations during which the swarm size is constant, ξ is the percentage reduction of the population while $\lfloor x \rfloor$ is the integer part of the variable x and $\lceil x \rceil = -\lfloor -x \rfloor$, where the symbolism used has been introduced in (Iverson, 1998).

3.2 Fitness Functions

In this work, the aforementioned procedure is applied *i)* to minimize an objective function properly defined to look for the design of the parallel feedforward compensator transfer function G_{PFC} in such a way that the augmented system Eq.7 becomes ASPR and *ii)* to minimize a fitness function used for the tuning of the invariant parameters $\mathbf{\Gamma}$ of the SAC scheme, see Eq. 6.

More in detail, *i)* the objective function, to be minimized with the aim of constructing the PFC transfer function G_{PFC} , is a modified norm of the discrepancy between the augmented y_a and actual y systems outputs undergoing a unitary step input excitation, u . The PFC transfer function is written as

$$G_{PFC}(s) = \kappa \frac{1}{b_1 s + 1} \tag{16}$$

being κ and b_1 the elements of the vector that defines the *i*-th particle $\mathbf{p}^i = [\kappa \quad b_1]^i$, while the objective function writes as

$$\mathfrak{S}_{PFC}(\mathbf{p}) = \phi(\mathbf{p}) \sqrt{\int_{T_W} [y_a(\mathbf{p}, t) - y(t)]^2 dt} \tag{17}$$

where $\phi(\mathbf{p})$ is a penalty function which equals 1 if G_a meets the ASPR conditions while $\phi(\mathbf{p})$ becomes numerically infinite otherwise. The minimization problem writes as

$$\begin{aligned} \min \quad & \mathfrak{S}_{PFC}(\mathbf{p}) \\ \text{s.t.} \quad & \mathbf{p}_{PFC \min} \leq \mathbf{p} \leq \mathbf{p}_{PFC \max} \end{aligned} \tag{18}$$

being minimum and maximum values of \mathbf{p} taken from Omori *et al.* (2013).

On the other hand, *ii)* the objective function to be minimized for tuning the SAC invariant parameters, $\mathbf{p}^i = [\Gamma_e \quad \Gamma_{xm} \quad \Gamma_{um}]^i$, writes as

$$\mathfrak{S}_{SAC}(\mathbf{p}) = \int_{T_W} [\alpha e^2(\mathbf{p}, t) + \beta \delta_e^2(\mathbf{p}, t)] dt \tag{19}$$

where α and β are weight parameters. The objective function Eq. 19 to be minimized looking for the best invariant controller parameters is thus the weighted sum of the integral of square (tracking) error and of the integral of the square elevator deflection. The former can be seen as a measure of the energy error and allows to give more importance to large errors with respect to small ones; the latter can be seen as a measure of the effort requested to the elevator to follow the reference signal and it allows to avoid the selection of parameters that would lead to high elevator deflection. In Eqs. 17 and 19, T_W is the time window extent over which the fitness value is computed. The invariant SAC parameters minimization problem writes as

$$\begin{aligned} \min \quad & \mathfrak{S}_{SAC}(\mathbf{p}) \\ \text{s.t.} \quad & \mathbf{p}_{SAC \min} \leq \mathbf{p} \leq \mathbf{p}_{SAC \max} \end{aligned} \tag{20}$$

The threshold values for the search of the SAC invariant parameters are set heuristically by conducting an a priori investigation of the problem.

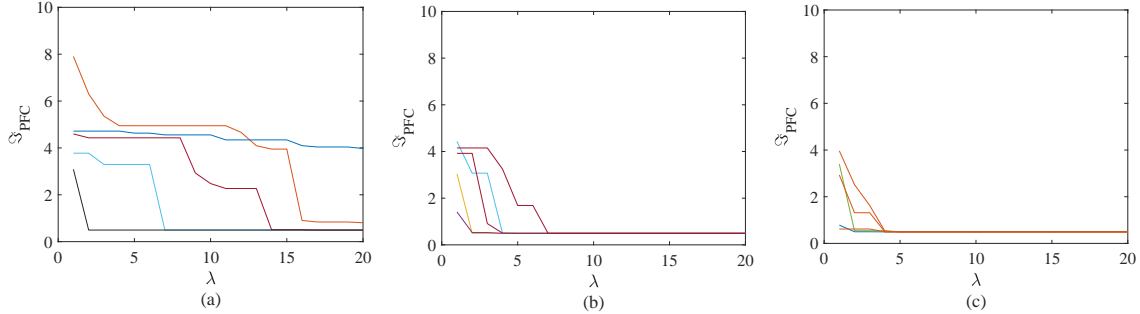


Fig. 2 ASPR - PFC fitness function convergence (five representative trends): (a) $P_{max} = 2$, (b) $P_{max} = 5$, (c) $P_{max} = 10$,

4. P_DSO tuning results

4.1 PFC design results

Numerical trial and error tests have been carried out to set the P_DSO coefficients for the problems under consideration. A simulation time window $T_W = 600$ s is used to compute numerically the fitness function Eq.17. Parameter set for P_DSO consists of: cognitive constant $c_c = 2.05$; social constant $c_s = 2.05$; minimum of inertia weight $\mu_{min} = 0.4$; maximum of the inertia weight $\mu_{max} = 0.9$; maximum number of iterations $\Lambda = 20$; time for population decline $\Delta = 3$.

The initial population size P_{max} is let increase to study the convergence behavior of the P_DSO tuning approach as compared with standard multi-start particle swarm optimizer (Orlando and Alaimo (2017)). To take into consideration the randomic nature of the P_DSO scheme, a total of 50 optimization have been run for each initial population swarm size. Five representative trends of the objective function Eq.17 are given in Figure 2 for any considered swarm size P_{max} evidencing that each swarm is randomly initialized and that, as the swarm size increases, the chosen number of iterations $\Lambda = 20$ is enough to ensure the convergence of the swarms.

P_DSO tuning results for the ASPR system are summarized in Table 1 in terms of values of the fitness function Eq. 17 at last iteration step $\lambda = \Lambda$. The minimum, maximum and median values of the objective function are shown in Table 1 along with the optimal parameters (κ, b_1) of the PFC function that let the augmented system Eq. 7 becomes ASPR, i.e. the parameters that give the minimum fitness function value.

Looking at the results related to $P_{max} = 2$, that is clearly an excessive small swarm, it can be noted that the minimum and median values are equal, meaning that at least 25 optimization procedures out of 50 manage to find the same minimum value of the objective function Eq. 17. Results for $P_{max} = 5$ and 10 confirm the minimum value of \mathfrak{S}_{PFC} that corresponds to $(\kappa, b_1) = (0.01, 1)$; the trend of the maximum value \mathfrak{S}_{Max} shows the good convergence behavior of the proposed P_DSO tuning scheme that is also evident by comparing results with the ones obtained by the standard PSO with multi-start scheme (the case with $\xi = 1$). Last comment on data collected in Table 1 refers to the speedup ratio defined as the

Table 1 ASPR - PFC tuning results by *P_DSO*. $\Lambda = 20$; $\Delta = 3$.

P_{max}	ξ	<i>speed up ratio</i>	\mathfrak{S}_{min}	\mathfrak{S}_{Max}	\mathfrak{S}_{median}	(κ, b_1)
2		0.55	4.947e-01	3.974e+00	4.947e-01	(1.00e-02, 1.00e+00)
5	0.50	0.34	4.947e-01	6.533e-01	4.947e-01	(1.00e-02, 1.00e+00)
10		0.27	4.947e-01	4.947e-01	4.947e-01	(1.00e-02, 1.00e+00)
10	1.00	-	4.947e-01	4.947e-01	4.947e-01	(1.00e-02, 1.00e+00)

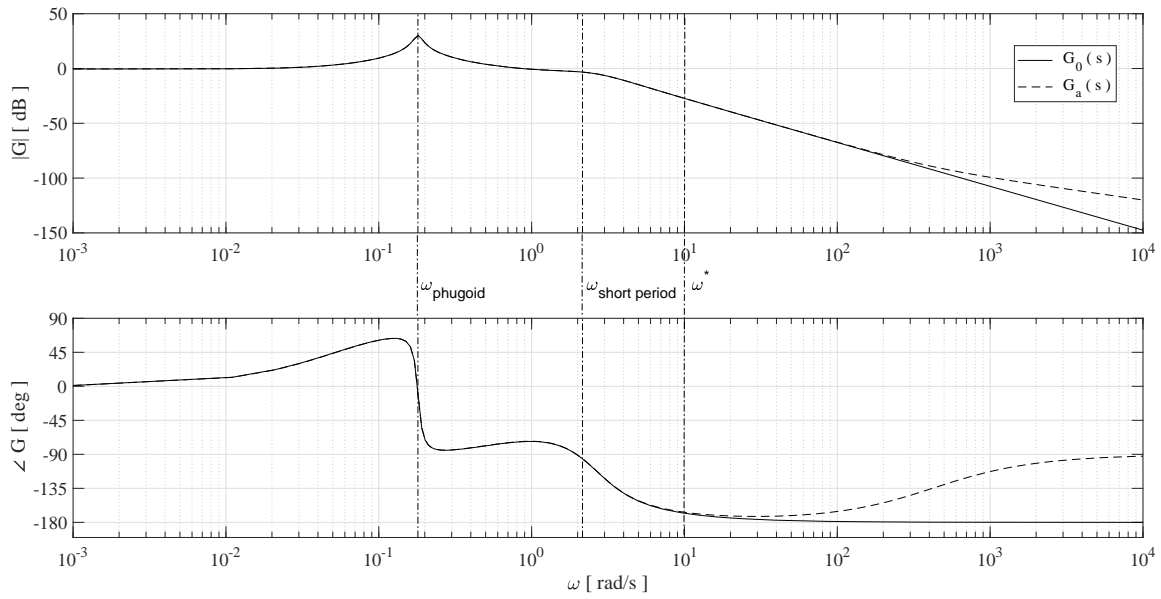


Fig. 3 Bode plot of the original and ASPR plants.

ratio between the computational time requested by *P_DSO* and the one of *PSO*. It is to note that, as the number of particle in the swarm increases, such ratio decreases and this means that the computational effort has been decreased when compared to *PSO* without affecting the global search capability.

The Bode plots of the original plant G_0 and of the augmented one G_a are graphically compared in Figure 3 showing that the added PFC transfer function does not modify the Bode diagram at low frequencies $0 \leq \omega \leq \omega^*$. This means that G_0 and G_a practically coincide and that PFC is small enough to not affect the plant in the frequency band where characteristic dynamics, airplane phugoid and short period modes, are present. However, the augmented plant is now ASPR and thus the Simple Adaptive Control can be applied.

4.2 SAC design results

The smoothed square wave Eq. 9 is passed as input to command the elevator deflection with the aim of tuning the invariant parameter Γ of the SAC scheme.

The amplitude of the square wave is $A_{ssw} = 2 \text{ deg}$, the circular frequency is $\omega_{ssw} = 0.1 \text{ rad/s}$ while smoothing parameter ρ_{ssw} is set to 100. The reference model Eq. 2 specifies

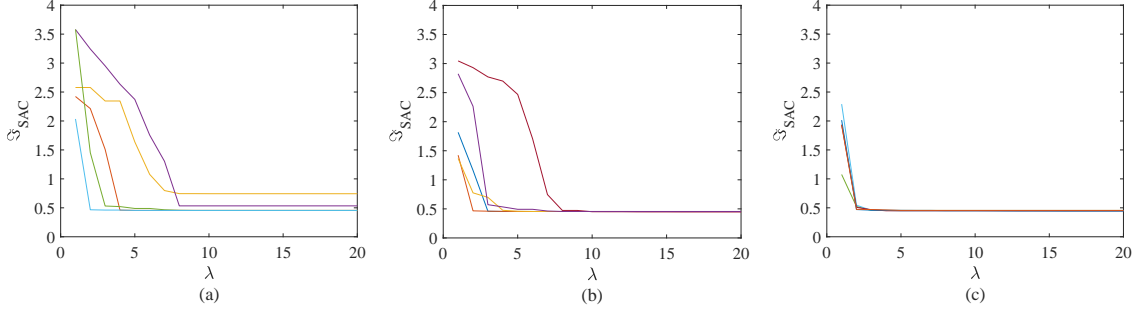


Fig. 4 SAC fitness function convergence: (a) $P_{max} = 5$, (b) $P_{max} = 10$, (c) $P_{max} = 20$,

Table 2 SAC tuning results by $P_{D}SO$. $\Lambda = 20$; $\Delta = 5$.

P_{max}	ξ	speed up ratio	\mathfrak{S}_{min}	\mathfrak{S}_{Max}	\mathfrak{S}_{median}	$(\Gamma_e, \Gamma_{xm}, \Gamma_{um})$
5	0.80	0.84	4.549e-01	7.434e-01	4.549e-01	(31.6, 0.001, 0.001)
10	0.80	0.75	4.467e-01	4.549e-01	4.549e-01	(25.3, 0.001, 0.269)
20	0.80	0.72	4.467e-01	4.549e-01	4.474e-01	(24.7, 0.001, 0.277)
20	1.00	-	4.467e-01	4.549e-01	4.549e-01	(25.0, 0.001, 0.272)

as $\{A_m, B_m, C_m\} = \{-1/0.05, 1/0.05, 1.00\}$. A simulation time window $T_W = 10 \text{ sec}$ is used to compute the objective function Eq. 19 to be minimized by the $P_{D}SO$ procedure. The parameters of the $P_{D}SO$ are set by trial and error tests and specify as: cognitive constant is $c_c = 2.05$; social constant is $c_s = 2.05$; 0.4 and 0.9 are the minimum and maximum values of the inertia weight μ ; the maximum number of iterations Λ is set to 20 while the time for population decline is $\Delta = 5$ while the minimum and maximum values of the search domain are set to 10^{-3} and 10^2 , respectively, for all SAC parameters. The convergence of the $P_{D}SO$ design scheme is studied by varying the initial size of swarm as $P_{max} = \{5, 10, 20\}$ and comparing results with the standard PSO procedure. A total of 50 optimizations have been run for each initial population size P_{max} and the convergence results of 5 representative fitness function Eq. 19 are graphically shown in Figure 4. From Figure 4 it can also be noted that the swarms are randomly initialized and converge in about 15 iterations, however swarms having $P_{max} = 5$ show a tendency to stuck to local minima.

Table 2 collects the tuning results at $\lambda = \Lambda$. It can be seen that the swarm with $P_{max} = 5$ does not find the minimum value of the fitness function if compared with the standard PSO. On the other hand, both the $P_{D}SO$ swarms with $P_{max} = \{10, 20\}$ are capable of finding the minimum value of the objective function Eq. 19 that equals $\mathfrak{S}_{SAC} = 0.04467$ however the results in terms of median show that an initial population of at least $P_{max} = 20$ should be used. In fact, the lowest value of the median ensures that the 20 particles swarm used with the proposed $P_{D}SO$ approach has good probability of finding the best parameters set for the SAC scheme employed. In this case the SAC invariant parameters obtained by the heuristic optimization are $\Gamma_e = 24.7$, $\Gamma_{xm} = 0.001$ and $\Gamma_{um} = 0.277$. Last, speedup ratio results confirm the reduced computational effort of the proposed $P_{D}SO$ with respect to the standard PSO .

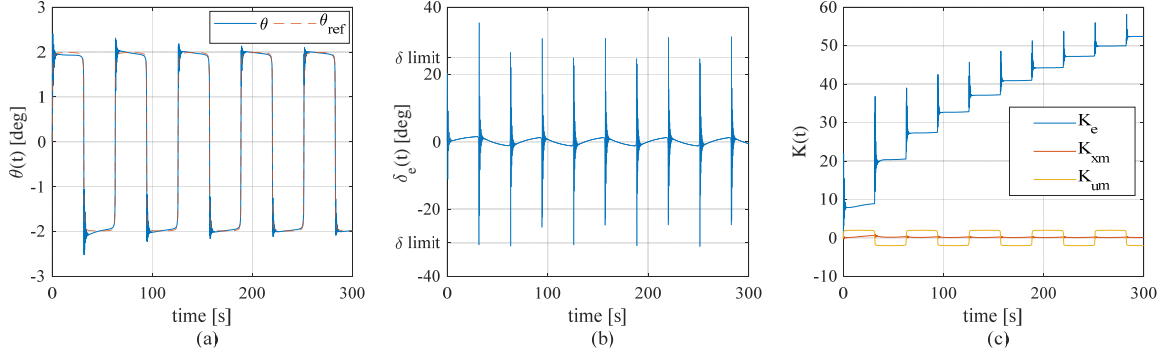


Fig. 5 Transient response of the nominal plant: $f_{ssw} = 0.1 \text{ rad/s}$; $\rho_{ssw} = 100$; $K_e(0) = 0$

5. Fault tolerant flight control system results

5.1 Case Study: Nominal plant

The pitch dynamic of the controlled aircraft is studied first. The controller parameters are the ones set by using the *P_DSO* procedure, namely $\Gamma_e = 24.7$, $\Gamma_{xm} = 0.001$ and $\Gamma_{um} = 0.277$. The reference state space model Eq. 2 that the plant has to follow for $T_w = 300 \text{ s}$ is $\{A_m, B_m, C_m\} = \{-1/0.05, 1/0.05, 1.00\}$. The smoothed square wave Eq. 9 is used as input to the reference model. The transient response of the controlled plant is calculated for the design case $f_{ssw} = 0.1 \text{ rad/s}$ and $\rho_{ssw} = 100$. Results are shown in Figure 5 in terms of pitch time history (a) and elevator deflection response (b); moreover in Figure 5(c) the time history of the adaptive SAC gains is given. By observing the results in terms of pitch angle it can be noted that the plant manages to follow the reference model but overshoots are present. The maximum value of such overshoot is 25% and occurs at about $t = 31 \text{ s}$, but, it is also interesting to note that overshoots reduce as time goes on. This suggests to assume that the controller is still trying to adapt to reference track after 300 s . By observing Figure 5(c) one can see that the previous assumption is confirmed by the trend of $K_e(t)$, that increases during the simulation time and it is not only affected by the reference signal variation. As last observation regarding the plant response in the design case, it is evidenced that elevator deflection reaches a maximum value of 31 deg at about $t = 31 \text{ s}$ and that the limiting elevator deflection values of $\{+25 \text{ deg}, -30 \text{ deg}\}$ (RUAG (2018)) are often violated.

Looking at Figure 5(c) one can note that zero initial conditions have been assumed to integrate Eq.6. This assumption is now removed for K_e , the initial value is set to 100 and the flight mechanics simulation is run, see Figure 6. From pitch angle time history shown in Figure 6(a) one can conclude that the controlled plant is now able to track perfectly the reference model and from Figure 6 it is also seen that the adaptive gains are now mainly influenced by the reference signal. Looking at the result in terms of elevator deflection, however, it is apparent that both the positive and the negative limit deflection angles are exceeded and this occurs only when the square wave slope changes. This suggests to modify the smoothed square wave law by reducing the sharpness of the variation. The parameter that governs the square wave smoothing radius is set to $\rho_{ssw} = 50$ and the flight dynamics

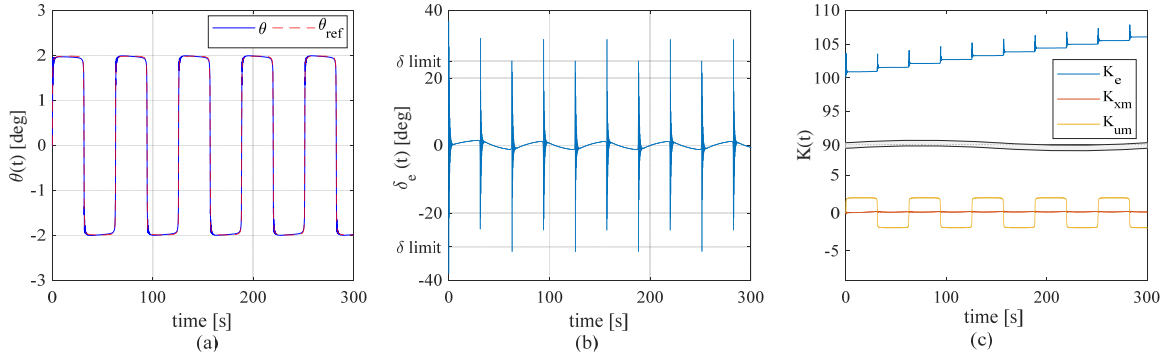


Fig. 6 Transient response of the nominal plant: $f_{ssw} = 0.1$ rad/s; $\rho_{ssw} = 100$; $K_e(0) = 100$

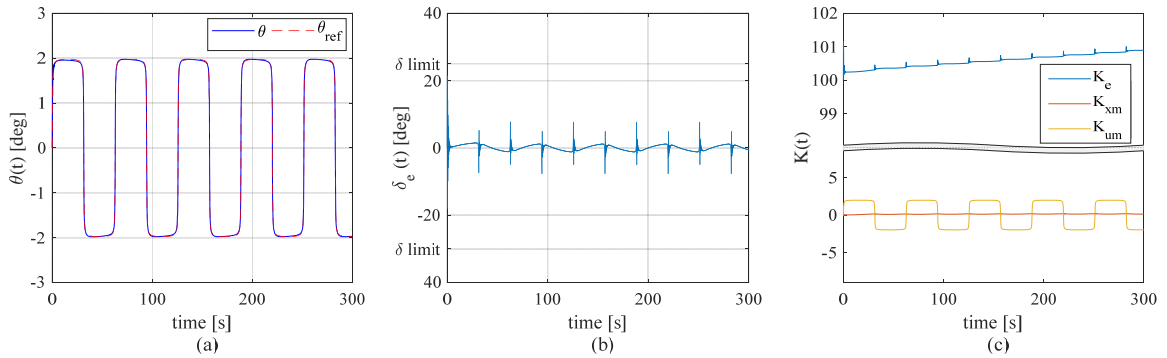


Fig. 7 Transient response of the nominal plant: $f_{ssw} = 0.1$ rad/s; $\rho_{ssw} = 50$; $K_e(0) = 100$

simulation is run. Figure 7 shows the obtained results and allow to see that the tracking capability is maintained while the peaks in the elevator deflection angle reduce dramatically with a maximum value of 20 deg at about $t = 0.1$ s.

The last parameters setting will be used to carry out simulation taking into account both elevator and stability failures.

5.2 Case Study: Elevator fault

The second study case is analyzed in the present section. It is aimed at investigating numerically the performance of the designed controller in the occurrence of a failure that reduces the effectiveness of the elevator. In particular three cases are investigated: *Case 1*, the fault occurs when the reference signal is maintained constant at the requested maximum pitch angle; *Case 2*, the fault occurs during the increasing and decreasing period of the commanded pitch angle; *Case 3* aims at studying the influence of the elevator effectiveness reduction.

5.2.1 Case 1: fault during maximum pitch angle

The first flight mechanics simulation assumes a 20% reduction of the elevator effectiveness, namely $\lambda_e = 0.8$, occurring at $t_{ef} = 142$ s. Figure 8 shows the numerical results in

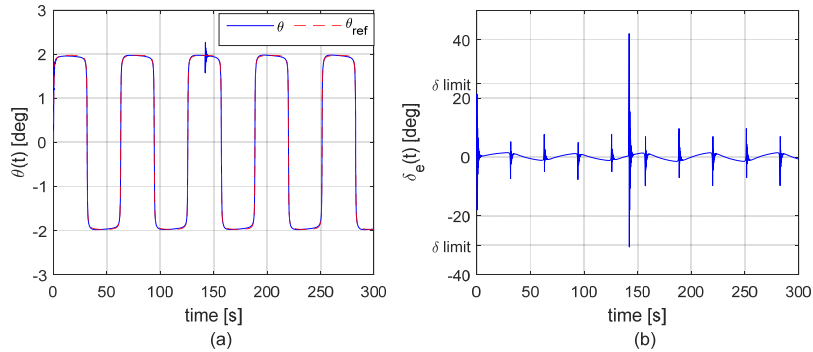


Fig. 8 Transient response of the controlled plant: elevator fault $\lambda = 0.8$ at $t = 142$ s.

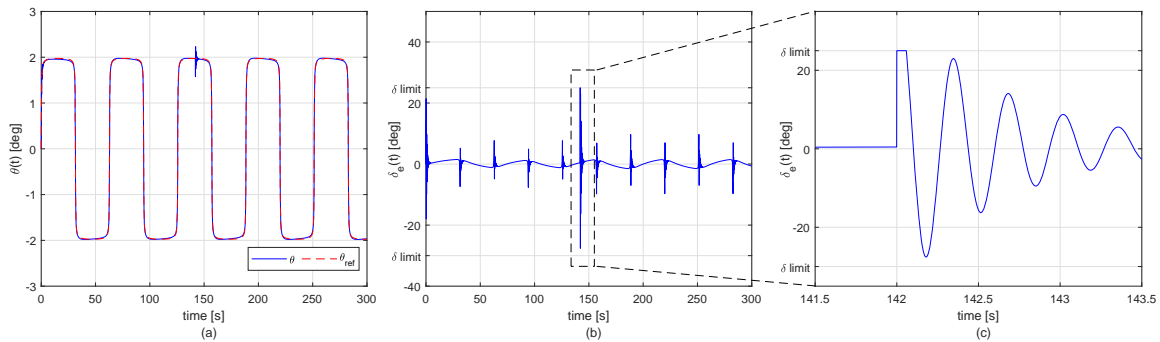


Fig. 9 Transient response of the controlled plant with saturation: elevator fault $\lambda = 0.8$ at $t = 142$ s.

terms of both pitch angle, compared to the requested reference model track, and elevator deflection time histories. By analyzing the aircraft pitch angle variation one can note that the plant is able to follow the reference signal even after the occurrence of the fault. The failure is revealed by the transient response of the plant, observable at $t = t_{ef}$, that is characterized by a percentage overshoot $PO = 21\%$, corresponding to a maximum shift from the reference of about 0.42 deg and a settling time $T_s = 3.1\text{ s}$. On the other hand, looking at the elevator deflection result, it is easily seen that limiting deflection values are overcome revealing that the linear model does not allow to accurately simulate the aircraft behavior in the analyzed fault condition. The limits on the elevator are thus modeled by introducing a function that saturates the elevator deflection at $\delta_{limit} = \{-30\text{ deg}, 25\text{ deg}\}$. This will allow to investigate the capability of the SAC, designed for the linearized plant, of controlling the plant in presence of nonlinearities.

Figure 9 shows simulation results obtained by modeling the saturation of the elevator deflection. Observing Figure 9(a) it appears that plant controlled by the SAC is able to follow the reference. Even in this case, at the instant of the failure, the pitch angle varies showing the same percentage overshoot, $PO = 21\%$, of the previous case that did not take into account the elevator deflection saturation. The settling time of such transient behavior

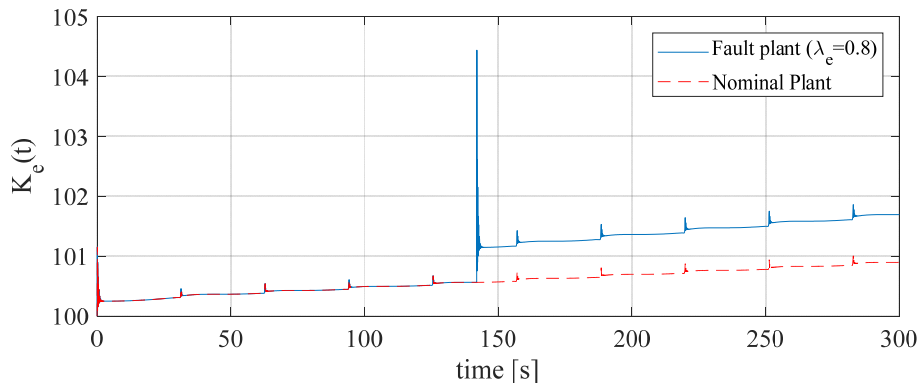


Fig. 10 Time history of the SAC error gain K_e of the nominal and fault plant.

is increased of 2 tenths of seconds with respect to the previous case. Thus it can be concluded that the presence of the saturation on the elevator deflection does not affect substantially the pitch dynamics of the controlled aircraft system. Looking at Figure 9(b) it stems that the elevator deflection amplitude is reduced and, in particular, it saturates to the upper limit of 25 deg for about 6 tenths of seconds. After the failure instant, the SAC modifies its parameter K_e , see Figure 10, in such a way to cope with the elevator effectiveness reduction recovering the capability of tracking the reference signal.

5.2.2 Case 2: failure during increasing/decreasing pitch angle

Let us now investigate the response of the controlled plant when the elevator fault occurs during the ascending or descending segments of the reference signal. More in detail, it is taken into account a failure that takes place at $t_e = 125.7 \text{ s}$ or at $t_e = 157.1 \text{ s}$; results are plotted in Figures 11. It is evident that in both cases the aircraft controlled by SAC behaves as the reference model and that the elevator deflection never reaches the saturation limits. In Figure 12 the trends of the adaptive error gain K_e is plotted in comparison with the undamaged case results. The existence of the failure is visible from the shifts of K_e from the nominal plant result (dashed line) that take place at $t = 125.7 \text{ s}$, for the solid line, and at $t = 157.1 \text{ s}$, for the dot-dashed line.

From the analyzed results, it can be concluded that the worst moment for the onset of a failure that reduces the elevator effectiveness is in those intervals of time during which the SAC error gain keeps constant.

5.2.3 Case 3: influence of elevator effectiveness

As last study, the influence of the parameter λ_e , that represents the severity of the failure, is investigated. It is assumed that the fault occurs at $t_e = 142$ and that the elevator effectiveness varies from $\lambda_e = 1$, when the plant is undamaged, to $\lambda_e = 0.1$, that represents a very serious event. Results are given in terms percentage overshoot PO and settling time T_s at the onset of the fault and are collected in Table 3. To analyze the controller capability of leading the damaged plant toward the reference signal after the failure, the integral square error ISE of the pitch angle is computed in the time interval $t \in [157.1; 282.2]$, that coincides

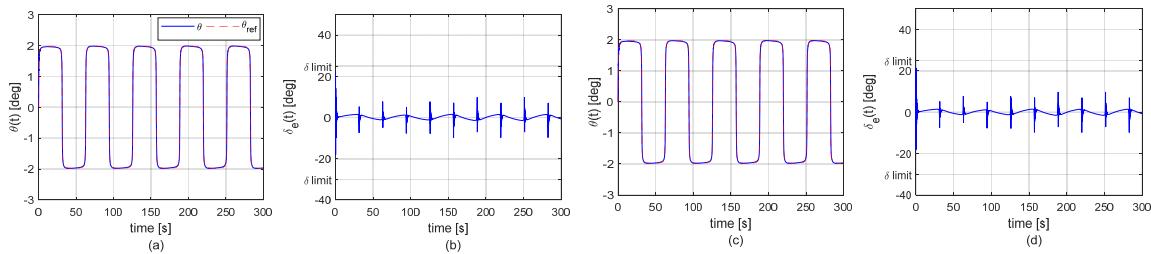


Fig. 11 Transient response of the controlled plant with saturation: (a) and (b) elevator fault $\lambda = 0.8$ at $t = 125.7$ s; (c) and (d) elevator fault $\lambda = 0.8$ at $t = 157.1$ s.

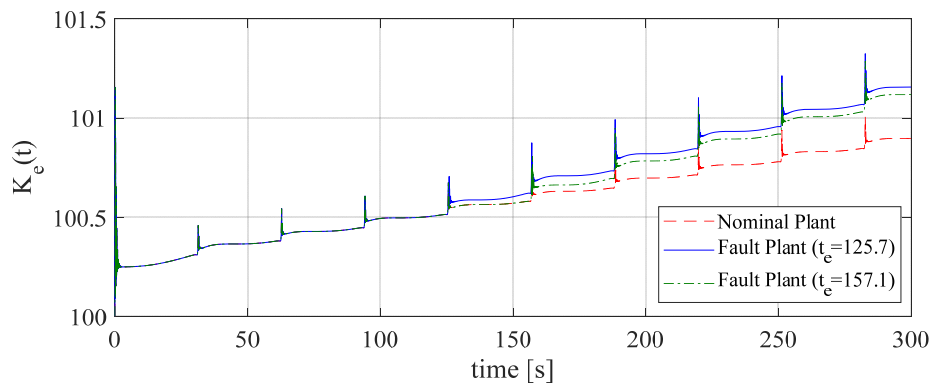


Fig. 12 Time history of the SAC error gain K_e of the nominal and fault plants.

with two period of the command signal. This quantity is also reported in Table 3. Observing such results it can be noted that as the failure severity increases the percentage overshoot increases almost linearly. The same stands for the settling time until $\lambda_e = 0.5$, infact as the damage severity becomes greater than the 50% the settling time increases more rapidly and then it keeps constant at about 4 s. It is to notice, however, that when the damage level exceeds the 70% the transient response changes as shown in Figure 13. Last, the integral square error increases linearly till $\lambda_E = 0.7$ and then its trend becomes nonlinear, as expected, for failure entity greater than 30%. From Figure 13 it also emerges that the proposed adaptive controller tuned by the *P_DSO* is capable of adapting well even in presence of a 60% elevator effectiveness reduction. In fact, after the failure instant, the proposed SAC leads the plant to track the reference signal. On the other hand, as λ_E becomes 0.3 or lower, the capability of the controlled plant to follow the model reference deteriorates progressively.

6. Conclusions

An adaptive flight control system capable of leading the aircraft pitch response even in presence of elevator failures has been presented in this work. The adaptive scheme is based on the Simple Adaptive Control approach and implements a Parallel Feedforward Compensator

Table 3 Influence of λ_e on the controlled plant response.

λ_e	1.0	0.9	0.8	0.7	0.6	0.5	0.4	0.3	0.2	0.1
PO	0.00	10.37	20.50	30.12	40.25	50.37	60.00	70.12	80.25	89.36
T_S	0.00	1.77	1.90	2.05	2.41	2.68	3.01	3.49	3.99	3.98
ISE	0.02	0.03	0.04	0.05	0.07	0.11	0.17	0.30	0.67	2.55

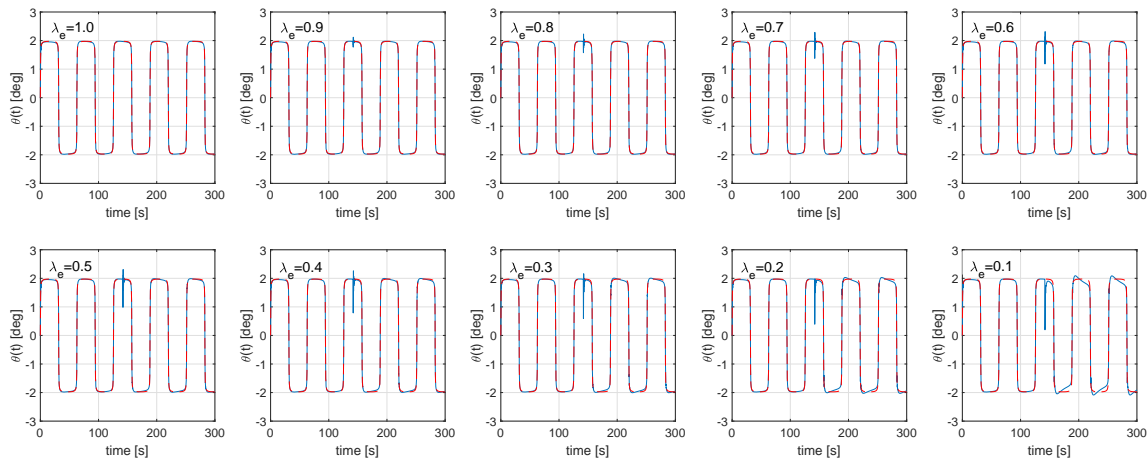


Fig. 13 Pitch transient results as function of elevator effectiveness.

to render the augmented system almost strictly passive. An alternative scheme based on a particle swarm optimization modification, called Population Decline Swarm Optimizer - P_{DSO} , has been employed to design the PFC and to select the invariant gains of the SAC. The proposed P_{DSO} has shown a global searching capability comparable with the standard PSO with less computational time effort. Numerical flight mechanics simulations have been carried out to study the effects of the command to the reference model on the undamaged aircraft transient response taking also into account physics limitation of the system. Results obtained by taking into account different type of elevator faults have shown the control systems ability to adapt automatically in such a way to let the damaged plant track the reference model. In particular, it has been found that the worst moment for the occurrence of the elevator effectiveness failure is during those periods characterized by a constancy of the adaptive gains. However, also in the aforementioned case, the proposed SAC controller tuned by the P_{DSO} optimizer is able to tackle the elevator effectiveness failure. What has been said stands valid even when the elevator rotation limits are taken into account and when the elevator effectiveness reduces of about 60% with respect to the undamaged case. The variation of the adaptive gains have been studied too, putting into evidence that the gain associated to the tracking error plays a prominent role with respect to the control and state feedforward gains. Moreover, it has been found that the time response of the simple adaptive controller can be improved by a proper selection of the initial value of the tracking error related adaptive gain.

References

- Barkana, I., Kaufman, H. and Balas, M. (1983), "Model reference adaptive control of large structural systems", *J. Guid. Control Dyn.*, **6**(2), 112-118. <https://doi.org/10.2514/3.8544>.
- Barkana, I. and Kaufman, H. (1985), "Global stability and performance of a simplified adaptive algorithm", *Int. J. Control*, **42**(6), 1491-1505. <https://doi.org/10.1080/00207178508933440>.
- Barkana, I. (1987), "On parallel feedforward and simplified adaptive control", in *Adapt. Syst. Control Signal Process.*, 99-104. <https://doi.org/10.1016/B978-0-08-034085-2.50021-3>.
- Barkana, I. and Kaufman, H. (1993), "Simple adaptive control of large flexible space structures", *IEEE T. Aerosp. Electron. Syst.*, **29**(4), 1137-1149. <https://doi.org/10.1109/7.259517>.
- Barkana, I. (2005), "Classical and simple adaptive control for nonminimum phase autopilot design", *J. Guid. Control Dyn.*, **28**(4), 631-638. <https://doi.org/10.2514/1.9542>.
- Barkana, I. (2014), "Simple adaptive control - a stable direct model reference adaptive control methodology - a brief survey", *Int. J. Adapt. Control Signal Proces.*, **28**(7-8), 567-603. <https://doi.org/10.1002/acs.2411>.
- Barkana, I. (2017), "On robustness and perfect tracking with simple adaptive control in nonlinear systems", *IFAC Papers On Line*, **50**(1), 4258-4263. <https://doi.org/10.1016/j.ifacol.2017.08.831>.
- Chen, F., Wu, Q., Jiang, B. and Tao, G. (2015), "A reconfiguration scheme for quadrotor helicopter via simple adaptive control and quantum logic", *IEEE T. Indust. Electron.*, **62**(7), 4328-4335. <https://doi.org/10.1109/TIE.2015.2389760>.
- Clerc M. and Kennedy J. (2002), "The particle swarm-explosion, stability, and convergence in a multidimensional complex space", *IEEE T. Evol. Comput.*, **6**(1), 58-73.
- Eterno, J. S., Weiss, J. L., Looze, D. P. and Willsky, A. (1985), "Design issues for fault tolerant-restructurable aircraft control", *Proceedings of the 24th IEEE Conference on Decision and Control*, Fort Lauderdale, Florida, U.S.A., December.
- Favre, C. (1994), "Fly-by-wire for commercial aircraft: the Airbus experience", *Int. J. Control*, **59**(1), 139-157. <https://doi.org/10.1080/00207179408923072>.
- Gai, W. and Wang, H. (2013), "Closed-loop dynamic control allocation for aircraft with multiple actuators", *Chin. J. Aeronaut.*, **26**(3), 676-686. <https://doi.org/10.1016/j.cja.2013.04.031>.
- Gertler, J. (2013), *Fault Detection and Diagnosis*, Springer, London, U.K., 1-7.
- Goodwin, G.C. and Sin, K.S. (2014), *Adaptive Filtering Prediction and Control*. Courier Corporation.
- Gransden, D.I. and Mooij, E. (2016), "Simple adaptive control of a satellite with large flexible appendages", *Proceedings of the 67th International Astronautical Congress*, Guadalajara, Mexico, September.
- Ioannou, P.A. and Sun, J. (1996), *Robust Adaptive Control*, Prentice-Hall, Upper Saddle River, New Jersey, U.S.A.
- Iverson K.E. (1962), "A programming language", *Proceedings of the May 1-3, 1962, Spring Joint Computer Conference. ACM.*, San Francisco, California, U.S.A, May.
- Landau, I.D., Lozano, R., M'Saad, M. and Karimi, A. (1998), *Adaptive Control (Vol. 51)*, Springer, London, U.K.
- Liu, Y., Ren, Z. and Cooper, J.E. (2018), "Integrated strategy for commercial aircraft fault-tolerant control", *J. Guid. Control Dyn.*, **41**(6), 1423-1434. <https://doi.org/10.2514/1.G003175>.
- Marinaki M., Marinakis Y. and Stavroulakis G.E. (2011), "Vibration control of beams with piezoelectric sensors and actuators using particle swarm optimization", *Expert Syst. Appl.*, **38**(6), 6872-6883.

- <https://doi.org/10.1016/j.eswa.2010.12.037>.
- Marti R. (2003), *Multi-Start Methods*, in *Handbook of Metaheuristic*, Springer, 355-368.
- Matsuki, H., Nishiyama, T., Omori, Y., Suzuki, S., Masui, K. and Sato, M. (2018), "Flight test of fault-tolerant flight control system using simple adaptive control with PID controller", *Aircraft Eng. Aerosp. Technol.*, **90**(1), 210-218. <https://doi.org/10.1108/AEAT-03-2016-0052>.
- Miller, R.H. and Ribbens, W.B. (1999), "Detection of the loss of elevator effectiveness due to aircraft icing", *Proceedings of the 37th AIAA Aeros ace Sciences Meeting and Exhibit*, Reno, Nevada, U.S.A., January.
- Min, L.I.U., Shijie, X.U. and Chao, H.A.N. (2012) "A backstepping simple adaptive control application to flexible space structures", *Chin. J. Aeronaut.*, **25**(3), 446-452. [https://doi.org/10.1016/S1000-9361\(11\)60401-9](https://doi.org/10.1016/S1000-9361(11)60401-9).
- Morse, W.D. and Ossman, A. (1990), "Model following reconfigurable flight control system for the AFTI/F-16", *J. Guid. Control Dyn.*, **13**(6), 969-976. <https://doi.org/10.2514/3.20568>.
- Nishiyama, T., Suzuki, S., Sato, M. and Masui, K. (2016), "Simple adaptive control with PID for MIMO fault tolerant flight control design", *AIAA Infotech@ Aerospace*, 0132.
- Noura, H., Sauter, D., Hamelin, F. and Theilliol, D. (2000), "Fault-tolerant control in dynamic systems: Application to a winding machine", *IEEE Control Syst.*, **20**(1), 33-49. <https://doi.org/10.1109/37.823226>.
- Omori, Y., Suzuki, S. and Masui, K. (2013), "Flight test of fault-tolerant flight control system using simple adaptive control with PID compensator", *Proceedings of the AIAA Guidance, Navigation, and Control and Co-located Conference*, Boston, Massachusetts, U.S.A., August.
- Orlando, C. and Alaimo, A. (2017), "A robust active control system for shimmy damping in the presence of free play and uncertainties", *Mech. Syst. Signal Process.*, **84**, 551-569. <https://doi.org/10.1016/j.ymsp.2016.07.038>.
- RUAG Aerospace Services GmbH (2018), "Dornier 228 Advanced Commuter (AC) Facts & Figures", dornier228.ruag.com.
- Rusnak I. and Barkana I. (2009), "SPR and ASPR untangled", *IFAC Proc. Vol.*, **42**(6), 126-131.
- Rusnak I., Weiss H. and Barkana I. (2014), "Improving the performance of existing missile autopilot using simple adaptive control", *Int. J. Adapt. Control Signal Process.*, **28**(7-8), 732-749. <https://doi.org/10.1002/acs.2457>.
- Sato M. (2006), "Flight test of model-matching controller for in-flight simulator MuPAL-alpha", *J. Guid. Control Dyn.*, **29**(6), 1476-1482. <https://doi.org/10.2514/1.25685>.
- Shi Y. and Eberhart R. (1998), "A modified particle swarm optimizer", *Proceedings of the IEEE World Congress on Computational Intelligence*, Anchorage, Alaska, U.S.A., May.
- Sobel, K., Kaufman, H. and Mabijs, L. (1979), "Model reference output adaptive control systems without parameter identification", *Proceedings of the 18th IEEE Conference on Decision and Control including the Symposium on Adaptive Processes*.
- Steinberg, M. (2005), "Historical overview of research in reconfigurable flight control", *Proc. Inst. Mech. Eng. Part G J. Aerosp. Eng.*, **219**(4), 263-275. <https://doi.org/10.1243>
- Takase, R., Entzinger, J.O. and Suzuki, S. (2017), "Interaction between a fault-tolerant flight control system using simple adaptive control and pilot's pitch control", *Proceedings of the 11th Asian Control Conference (ASCC)*, Gold Coast, Australia, December.
- Tao, G. (2003), *Adaptive Control Design and Analysis*. John Wiley and Sons.
- Tokunaga, D., Masui, K. and Suzuki, S. (2015), "Flight evaluation of fault-tolerant control system

- using simple adaptive control method”, *Procedia Eng.*, **99**, 1035-1043.
- Ulrich, S. and de Lafontaine, J. (2007), “Development of a novel adaptive control algorithm for a fighter aircraft”, *Proceedings of the AIAA Guidance, Navigation and Control Conference and Exhibit*, Hilton Head, South Carolina, U.S.A., August.
- Wise, K.A., Brinker, J.S., Calise, A.J., Enns, D.F., Elgersma, M.R. and Voulgaris, P. (1999), “Direct adaptive reconfigurable flight control for a tailless advanced fighter aircraft”, *Int. J. Robust Nonlin. Control*, **9**(14), 999-1012. [https://doi.org/10.1002/\(SICI\)1099-1239\(19991215\)9:14](https://doi.org/10.1002/(SICI)1099-1239(19991215)9:14)
- Zhang, Y. and Jiang, J. (2003), “Fault tolerant control system design with explicit consideration of performance degradation”, *IEEE T. Aerosp. Electron. Syst.*, **39**(3), 838-848. <https://doi.org/10.1109/TAES.2003.1238740>.
- Zhang, Y.M. and Jiang, J. (2002), “Active fault-tolerant control system against partial actuator failures”, *IEE Proc. Control Theor. Appl.*, **149**(1), 95-104. <https://doi.org/10.1049/ip-cta:20020110>.
- Zhang, Y. and Jiang, J. (2007), “Issues on integration of fault diagnosis and reconfigurable control in active fault-tolerant control systems”, *Fault Detect. Supervision SafetyTech. Proces.*, 1437-1448. <https://doi.org/10.3182/20060829-4-CN-2909.00240>.
- Zhang, Y. and Jiang, J. (2008), “Bibliographical review on reconfigurable fault-tolerant control systems”, *Ann. Rev. Control*, **32**(2), 229-252. <https://doi.org/10.1016/j.arcontrol.2008.03.008>.

AP